

EFFECT OF PARTIAL HEATING ON NATURAL CONVECTION IN A CUBICAL CAVITY WITH AN INTERNAL OBSTACLE: A URANS STUDY

C. Katsamis^{1,2}, D.R. Wilson², T.J. Craft² and H. Iacovides²

¹EDF Energy R&D UK

² Thermo-Fluids Research Group, Department of MACE, The University of Manchester, UK
constantinos.katsamis@manchester.ac.uk

1. Abstract

The performance of advanced RANS turbulence models using different near-wall treatments is assessed in the computation of a natural convection flow occurring in a cubic cavity with a partially heated inner obstacle. The flow field has a Rayleigh number of 1.4×10^9 at which recent experimental data have been published. The time dependent 3D computations apply eddy-viscosity ($k - \varepsilon, k - \omega$ based) and advanced Reynolds stress transport models (EB-RSM). The predictions returned from a recently developed variant of the analytical wall function combined with either high-Re or low-Re $k - \varepsilon$ formulation are assessed. The low-Re $k - \varepsilon$ AWF combination leads to substantial predictive improvements of the Nusselt number levels on the active walls despite the coarse grid resolution adopted.

2. Introduction

Natural convection flows are relevant for industrial unsteady heating or cooling applications in which the fluid is driven by the density variations induced by a temperature difference. The flow phenomena generated in such flows have been widely studied experimentally and numerically to advance current understanding. Numerical modelling follows mostly RANS, LES and hybrid RANS-LES approaches, with the results being compared against either experimental or DNS of simple square cavity configurations [1-3]. Recently, high quality experimental data of a more challenging square cavity configuration with a heated obstacle shown in Figure 1 have been published by Weppe et al. [4] which aims to provide insight into the flow encountered in the vehicle engine's compartment. The configuration shown in Figure 1, comprises a square cavity cooled on the left and right vertical walls with a partially heated inner obstacle. Despite being a geometrically simple configuration, the near wall heat transfer effects and fully turbulent boundary layers make the use of the standard log-law wall function approach inappropriate, with researchers favouring low-Re RANS or LES approaches that fully integrated the transport equations down to the wall. However, the high level of unsteadiness and the low turbulence levels at $Ra \sim 10^9$ tend to challenge the low-Re RANS schemes in maintaining the flow turbulent, motivating the use of more advanced approaches such as LES or Hybrid-RANS LES as shown in the comparisons of the 17th SIG ERCOFTAC workshop. Amongst the results presented, the more recently developed advanced wall function approach (AWF) of [1, 2], which adopts a subgrid to solve the near wall momentum and energy equations, has been proved quite cost effective and provided sufficient accuracy in predicting the near-wall shear stress and heat flux distribution. Thus, the present study aims to test the effectiveness of URANS predictions, which are commonly adopted in industry, and to compare their results with those obtained using the advanced near-wall treatment of [1, 2], in reproducing the overall flow and thermal behaviour in the cubic cavity of Weppe et al. [4].

3. Numerical method and case description

The heated section of the cavity configuration shown in Figure 1, generates the upward flow motion. The fluid is assumed to be air with Prandtl number of 0.71 and the flow is governed by:

$$Ra_H = (g\beta(T_h - T_c)(H_{bloc})^3)/\nu\alpha = 1.4 \times 10^9 \quad (1)$$

The boundary conditions for the three active walls are set as isothermal, with the inner wall of the obstacle being set at temperature 32K higher than the outer walls, so to match the experimental Ra . The rest of the walls were assumed as adiabatic. The two-equation $k - \varepsilon$ and $k - \omega$ STT eddy viscosity models have been adopted for approximating the effects of turbulence using the eddy viscosity assumption. The different forms of the $k - \varepsilon$ assessed include the high-Re Launder and Spalding model combined either with the log-law based

*Corresponding Author: constantinos.katsamis@manchester.ac.uk

or the Analytical Wall Function of [1,2], a combination of AWF with low-Re Launder Sharma near-wall damping terms, and the low-Re Launder Sharma scheme that integrates the equation down to the wall. For all the wall function combinations, a uniform coarse grid with ~ 1 million cells and a y^+ value of the near-wall cells in the range of 5-15 has been adopted, whereas for the low-Re LS $k - \varepsilon$, $k - \omega$ *STT* and EB-RSM, a mesh with 5 million cells, satisfying a $y^+ < 1$ core the near-wall cells, were utilized (see Figure 2). The open-source CFD solver Code_Saturne v5.0.8/6.0.0 which employees the Finite Volume method with a collocated storage arrangement is used for the solution of the discretised momentum, mass and energy transport equations. Second order discretization schemes have been used for the convective fluxes of each transport equation and the 1st order semi-implicit scheme with a $\Delta t = 0.025$ s for the time discretization.

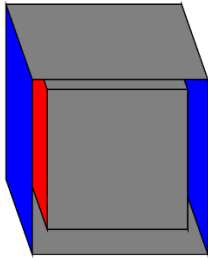


Figure 1: 3D schematic of the experimental configuration of the cubic cavity of [4].

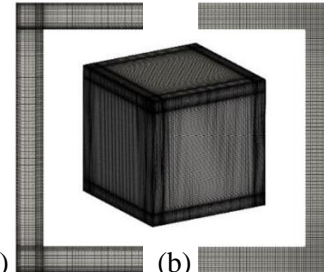
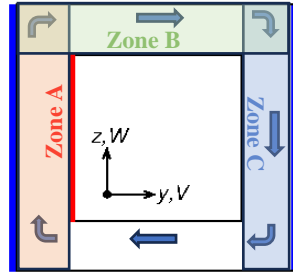


Figure 2: Grid design for the (a) low- and the (b) high- Re models for the 3D computations.

4. Results and Discussion

The predicted non-dimensional temperature ($\theta = (T - T_0)/\Delta T$) and velocity ($W/(\alpha/H_{bloc} * \sqrt{Ra_H})$) profiles from all the models along the height of the heated channel of the cavity are shown in Figure 3. The different model predictions are shown to largely agree with the scanned data. It can be observed that vertical velocity begins with a low average value near the bottom region and becomes stronger as the fluid ascends. Differences from model to model are observed at that location, $z = 0.1$, where the largest deviation compared to the scanned data appears for both velocity and temperature. The peaks of the vertical velocity profiles beyond this region, which suggest the development of the boundary layer are not captured well by the wall function models due to the low grid resolution there. The cold wall Nusselt number comparisons, presented in Figure 4, show a peak at $z=0.9$, the location where there is a recirculation region. This recirculation region is generated at the top left corner of the cavity, as shown in Figure 5, from the predicted streamlines of all models, being inline with the findings of the experiment. This recirculation region is an outcome of a buoyant oscillating jet that causes the flow to follow two different directions, with its effects being diminished as the flow circulates around the channels of cavity. The LS $k - \varepsilon$ (AWF) which includes the low-Re damping terms, returned a hot wall Nu (Figure 6) that matches closely the scanned data, suggesting that the prediction of wall heat flux from the subgrid is quite satisfactory. It worth noting that the high-Re wall function models, with far more modest grid requirements maintain a turbulent flow whereas the wall resolved models, with a much finer near-wall grid resolution tend to laminarise the flow.

5. Conclusions

Transient RANS simulations have been presented of the natural convection flow within a cubic cavity that contains a partially heated inner obstacle, and comparisons of the results made against the experimental data of Weppe et al. [4]. Overall, the mean temperature and velocity field are captured reasonably well by the various models tested in the heated region, even by those returning very low turbulence levels (EB-RSM, LS $k - \varepsilon$). The study highlights the difficulties of RANS models in returning the correct balance between modelled turbulence and resolved large-scale instability at such fairly low Rayleigh. The full paper will include a more detailed discussion of the flow physics, analysis of the flow and thermal field behaviour in the top and unheated region of the cavity and the predictions of the different models.

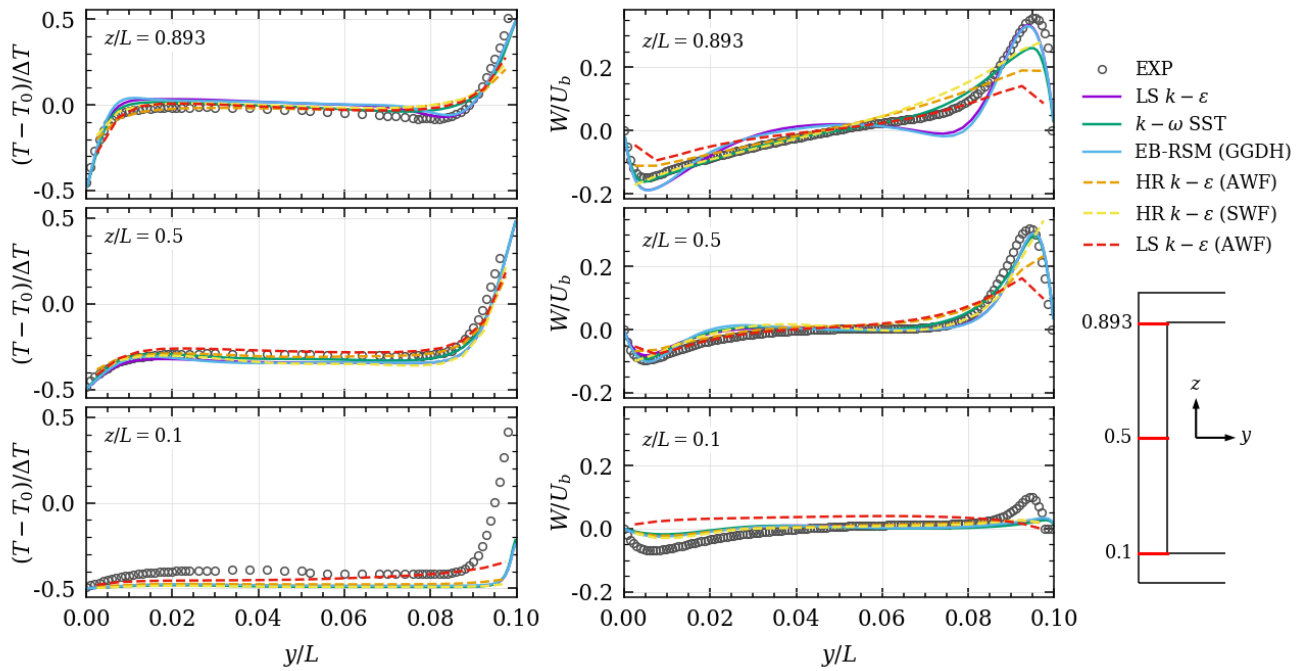


Figure 3: Non-dimensional temperature and w velocity profiles along the heated channel region of the cavity.

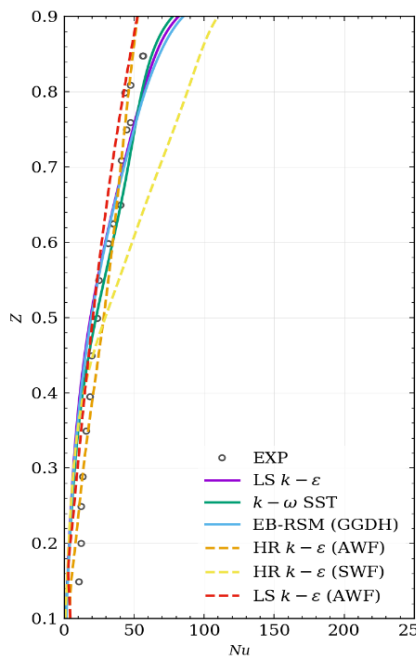


Figure 4: Cold wall Nusselt number model comparisons.

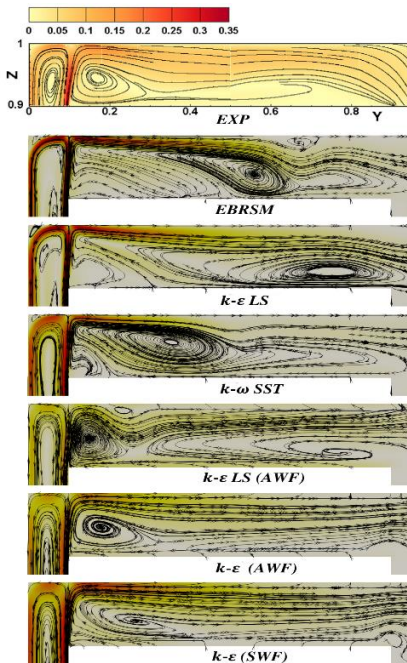


Figure 5: Velocity magnitude and streamlines from the top half of the cavity.

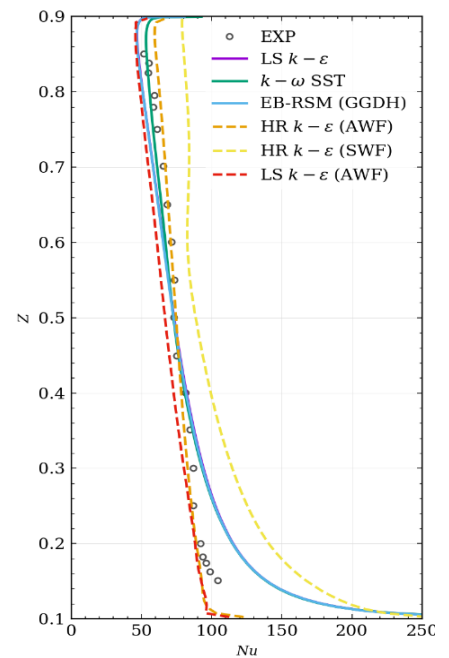


Figure 6: Hot wall Nusselt number model comparisons.

References

[1] Katsamis C., Craft T. J., Iacovides H., Uribe J. C. (2022). Use of 2-D and 3-D unsteady RANS in the computation of wall bounded buoyant flows, *International Journal of Heat and Fluid Flow*, 93, 108914.
 [2] Katsamis C., Craft T., Iacovides H. (2024) Highly resolved LES and URANS computations of a differentially heated square cavity. *International Journal of Thermofluids*, 21, 100564.
 [3] Sebilliau F., Issa R., Lardeau S., Walker P. S. (2018). Direct Numerical Simulation of an air-filled differentially heated square cavity with Rayleigh numbers up to 1011. *International Journal of Heat and Mass Transfer* 123, 297-319.
 [4] Weppe A., Moreau F., Saury D. (2022). Experimental investigation of a turbulent natural convection flow in a cubic cavity with an inner obstacle partially heated, *International Journal of Heat and Mass Transfer*, 194, 123052.